Available online at www.sciencedirect.com
SCIENCE DIRECT®
Journal of Sound and Vibration 281 (2005) 565–591
JOURNAL OF SOUND AND VIBRATION
www.elsevier.com/locate/jsvi

Nonlinear dynamics of cable stays. Part 2: stochastic cable support excitation

C.T. Georgakis*, C.A. Taylor

Department of Civil Engineering, Earthquake Engineering Research Centre, University of Bristol, Queens Building, University Walk, Bristol BS8 1TR, UK

Received 10 August 2001; accepted 27 January 2004
Available online 30 September 2004

Abstract

In this paper, an extensive behavioural study of cable vibrations, induced by in-plane stochastic cable-stayed structural vibrations, is made. Finite element modelling (FEM) and analysis (FEA) is used to determine in-plane and out-of-plane cable displacements induced by stochastic cable end displacements. The effects of stochastic cable support displacements, with abrupt and gradual transients, are studied. Regions of large-amplitude cable vibrations, induced by stochastic cable end displacements, are compared with those found from sinusoidal cable end displacements. The results show that, together with important similarities in cable response, there are also important differences in cable response between sinusoidal and stochastic cable support excitation. Differences in cable response amplitudes are found and discussed. It is also found that "cable-stiffening" occurs, for specific cable excitation parameters, as it does for sinusoidal cable support excitation, but to a lesser extent. Throughout the analyses, maximum cable stresses are calculated and, in some cases, are found to be near that required for cable material yielding.

1. Introduction

Over the past 50 years there has been an ever-growing interest in the dynamics of cables. This has been mainly due to the large increase in the design and construction of various types of cable

*Corresponding author. Skovagervej 7, Holte, DK-2840, Denmark.
E-mail address: cg@force.dk (C.T. Georgakis).

0022-460X/$ - see front matter © 2004 Elsevier Ltd. All rights reserved.
doi:10.1016/j.jsv.2004.01.023

Nomenclature

l	total length of cable
t	dimensional time
x	distance along the cable
E	material modulus of elasticity
A	cross-sectional area of cable
g	gravitational acceleration
θ	angle of inclination of the cable
D	cable diameter
μ	mass per unit length of cable
M	mass of cable support or mass–spring–dashpot damper system
N_c	cable tension at mid-span
ε_{xx}^{init}	cable initial strain
Δ_{max}	maximum vertical cable support displacement
Δ_{max}^{bridge}	maximum expected vertical bridge (cable end) displacement
$\Delta(t)$	time-dependant displacement of cable support or mass–spring–dashpot damper system
Δ_{rms}	rms displacement value
ω_1^{nl}	in-plane first circular frequency due to cable sag
ω_k	cable's modal frequencies
ω	circular frequency of cable support or mass–spring–dashpot damper system
ω_d	damped circular frequency of cable support or mass–spring–dashpot damper system
Ω	cable support excitation frequency
ξ_{pk}	aerodynamic parallel to wind damping ratios of cable
ξ_{nk}	aerodynamic normal to wind damping ratios of cable
ξ	damping ratio
β	nondimensional cable support displacement parameter
$p(\tau)$	white noise signal function
u	in-plane cable displacement
ρ	density of air
C_d	cable drag coefficient
V	wind velocity
e	relative energy coefficient
σ_y, σ_{max}	cable material yield stress and maximum observed stress respectively
E_k^{stoch}, E_k^{sin}	stochastic and sinusoidal support excitation kinetic energies, respectively
E_i^{stoch}, E_i^{sin}	stochastic and sinusoidal support excitation relative input energies, respectively

Definition of coefficients

$$\omega_1 = (v_t\pi)^2$$
$$v_t^2 = N_c/(\mu g l \cos\theta)$$
$$v_l^2 = EA/(\mu g l \cos\theta)$$

supported structures. Until the early 20th century, high tensile strength steels were unavailable for the construction of large engineering structures such as cable-stayed bridges. It was only with the introduction of these steels that engineers were finally able to design and create large cable-supported structures.

There are now thousands of large cable-supported structures world-wide. Many of these structures, although, occasionally exhibit undesirable large amplitude cable vibrations. Most small to medium amplitude cable vibrations can be attributed to wind or wind-rain/ice-induced mechanisms, through flutter, buffeting, vortex-shedding or galloping [1–4]. These mechanisms are fairly well understood and engineers are continuously developing effective countermeasures, for the suppression of these vibrations. The mechanisms behind some of the cable vibrations, though, especially large-amplitude cable vibrations, are still not completely understood. In an attempt to understand these vibrations, researchers have focused on the cable's linear and nonlinear dynamics.

Irvine and Caughey [5,6] studied the free vibrations of cables, using linear equations of motion, while Takahashi and Konishi [7,8] managed to locate unstable regions, in which cables exhibit large in-plane and out-of-plane vibrations, using nonlinear equations of motion. Others [9–14] have followed with similar studies using sinusoidal time-varying cable support displacements. Georgakis et al. [15] studied displacement levels and varying initial conditions to see what effect these had on the dynamics of a cable, while at the same time, looking at periodic, quasi-periodic and chaotic cable vibrations.

In all of the above-mentioned theoretical studies, a cable of finite length, with a uniformly distributed mass and a relatively small sag-to-span ratio, is examined, always under the influence of sinusoidal cable end displacements. The cable is placed horizontally between two supports at the same or at different levels. Three partial differential equations (PDEs), describing the motion of the cable along its axis, in-plane and out-of-plane are transformed into ordinary differential equations (ODEs) using the Galerkin or other similar de-coupling methods [7–15]. The PDEs are de-coupled when the acceleration term of the equation of motion, describing the cable's along-axis excitation, is equated to zero. The derived nonlinear equations of motion consider the parabolic shape of the cable under the influence of gravity. Finally, approximate solutions for the ODEs are found and the results are, when possible, compared to observations from actual and experimental cable vibrations.

In none of the previous studies has the effect of stochastic cable support excitation been studied in any detail, though. The aim of the study presented here is to provide further insights into the dynamics of cables subjected to stochastic support excitation.

All of the analyses presented here were performed through FEM with readily available software packages. The nonlinear equations of motion of the hanging cable [15] were not deemed appropriate for these analyses, as their integration for stochastic excitation proved to be uneconomical. It was assumed throughout the analyses that the cable behaved elastically and, as such, the total cable stresses were continuously monitored.

Examination of the results, obtained from the stochastic cable support excitation, show that stochastic excitation can induce very different cable vibrations from those that one might expect from a sinusoidal cable support excitation. A full comparison of the results is presented in the following sections.

Note that a full statistical study regarding the stochastic time-histories and the cable's response was not carried out, as the purpose of this work was not to examine all possible stochastic time-histories or the probability of a specific cable response outcome. It was clear from the onset of this work that a general picture of the cable's response to a stochastic end displacement could be achieved with a limited number of input time-histories.

2. Selection of cable parameters

Due to the infinite number of damping values and angles of inclination that a cable may take, several values were selected to represent typical cables on existing structures, these mainly being cable-stayed bridges. These were then analysed and results were examined. It was evident from the analysis that zones of large-amplitude cable vibrations, do tend to change with varying angles of inclination, when the geometric

nonlinearity of the cable lessens, as the angle of inclination moves towards 90°. Also, the onset of these regions of large-amplitude cable vibrations required higher amplitudes of cable end excitation as the damping of the cable increases, as observed by Mathieu using simplified equations [16]. It was decided that, due to the variety of results, one cable with one angle of inclination and two (2) different damping levels would be presented here as a typical example of an actual cable-stay. The selection of specific parameters leaves scope for further research, to investigate a fuller range of cable parameters.

The cable chosen is similar to one of the longest stays of the cable-stayed Second Severn Crossing bridge, UK, and will be referred to as cable A. Cable A has a length of 244.4 m, a steel cross-sectional area of 11250 mm^2 and an angle of inclination of 20.3°. The cable's structural damping has been estimated by Macdonald [17], from on-site measurements, to be about 0.05%. Its mass per unit length is 123.24 kg/m. A typical cable stay will have an average damping value of about 0.1% [17,18].

To suit future laboratory experiments, these quantities have been scaled-down by a ratio of 1:114. All of the structural quantities are scaled by this ratio except for the mass per unit length quantities, which were scaled so that the cable under examination has scaled natural frequencies equal to those of the bridge stay. The scaled quantities were then used for the FEA. Also, it has been estimated that the total static tension of the prototype cable-stay was about 30% of that required for material yielding [17]. This quantity is also scaled so that the total tension in the scaled cable is equal to approximately 30% of the force required for material yielding.

3. FEA software and model

Finite element modelling (FEM) and analysis was realised using the SOLVIA Finite Element System [19]. The FEM comprises of ten, linked, truss elements (Fig. 1), which create a scaled cable, 2.086 m long. Both cable end supports are fixed. The static tension of the cablewas 91.215 N and its cross-section area is $2.027 \times 10^{-7}\,m^2$. The static tension of the cable is due to the cable's own weight and a pre-tension that was imposed by applying an initial strain of $\varepsilon_{xx}^{init} = 0.002$. The mass of 0.4047 kg/m is uniformly distributed along the cable and the cable has a material modulus of elasticity of $E = 1.95 \times 10^{11}\,N/m^2$. Nonlinear analysis was used for the static analysis, which determined the maximum cable sag to be 0.022094 m (Fig. 1). Nonlinear dynamic analyses were then performed for the analyses of the cable's responses to various stochastic support excitations. The cable's first natural in-plane circular frequency ω_1^{nl} can be theoretically calculated, according to Perkins [14], by finding the roots of the equation

$$\tan\frac{\omega_1^{nl}}{2v_t} - \frac{\omega_1^{nl}}{2v_t} + \frac{(\omega_1^{nl}v_t)^3}{2v_l^2} = 0, \tag{1}$$

where coefficients v_t and v_l are defined in the nomenclature.

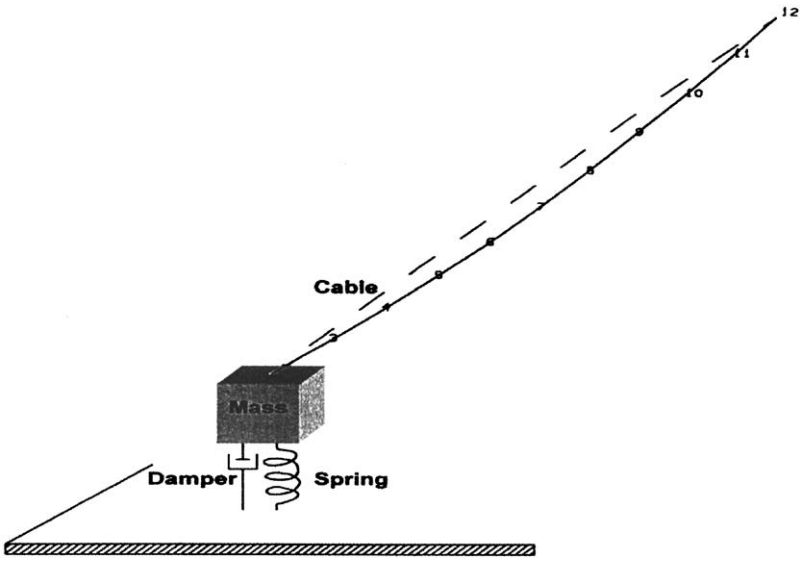

Fig. 1. Single-degree-of-freedom structure with mass, spring and dashpot damper attached to cable with 10 linked truss elements.

Finite element modal analysis, following a nonlinear static analysis, found that the first in-plane nonlinear natural frequency of the cable is 4.061 Hz. The theoretical first in-plane nonlinear natural frequency of the cable, as calculated by Eq. (1) is 4.086 Hz.

4. Stochastic support excitation

4.1. Synthetic stochastic time-histories

It was considered important that the stochastic excitation, which was to be imposed on the cables, be representative of a prototype stochastic time-history that might be imposed on a stay by a full-scale cable structure such as a cable-stayed bridge. Even though an approximation, cable structures, such as telecommunications masts and cable-stayed bridges, are subject to random wind forces, which have time-histories that are very similar to random normal distribution white noise signals, for the low-frequency bandwidth under examination. A cable-stayed bridge or other similar structure will act as a signal filter, by filtering wind signals (or white noise signals) through its own structural characteristics. The resulting dynamic response input will be the actual response of the structure to the wind load. This filtered signal or structural response can then be used as a stochastic time-history (stochastic support excitation) for the examination of a cable's nonlinear response to that time-history. As the wind will have varying characteristics, such as wind speed and wind direction, the force acting on the structure will also have varying characteristics. These will excite the structure at different frequencies with varying amplitudes of force. In most cases the

wind will have the effect of exciting one structural frequency (or mode) more than others [17]. As such, it was deemed appropriate that the stochastic signals, created for the examination of the nonlinear response of a cable, be equivalent to the response of the structure that the cable is supporting with specific frequency content. Cable-structure interaction was not examined herewith, but will be presented in a subsequent paper.

To create these synthetic time-histories, a cable-stayed bridge with specific structural characteristics was considered and modelled as a linear mass–spring–dashpot damper system (Fig. 1). A normal distribution white noise signal was imposed as a wind force on this system. The response $\Delta(t)$ of the bridge (linear system) was calculated through the Duhamel integral [20]. The integral for an under-critically damped system will be

$$\Delta(t) = \frac{1}{M\omega_d}\int_0^t p(\tau)\sin\,\omega_d(t-\tau)\exp[-\xi\omega(t-\tau)]\,\mathrm{d}\tau. \tag{2}$$

As the response of the structure is normalised to a unit of *one*, the mass, M, of the structure becomes irrelevant in the calculation of the system's response. The circular frequency Ω, which is the excitation frequency parameter used for the examination of the cable, is equated to the circular frequency of the linear system. Thus

$$\omega = \Omega. \tag{3}$$

The damped frequency of the system will be

$$\omega_d = \omega\sqrt{1-\xi^2}, \tag{4}$$

where ξ is the damping ratio of the system. $p(\tau)$ is the normal distribution white noise signal.

Following [20], Eq. (2) can be written as

$$\Delta(t) = A(t)\sin\,\omega_d t - B(t)\sin\,\omega_d t, \tag{5}$$

where

$$A(t)_n = A(t)_{n-1}\,\exp(-\xi\omega\,\delta\tau) + \frac{\delta\tau}{\omega_d}[y^a_{n-1}\exp(-\xi\omega\,\delta\tau)] \tag{6}$$

and

$$B(t)_n = B(t)_{n-1}\,\exp(-\xi\omega\,\delta\tau) + \frac{\delta\tau}{\omega_d}[y^b_{n-1}\exp(-\xi\omega\,\delta\tau)] \tag{7}$$

and where

$$y^a_n(t) = p(\tau)\sin\,\omega_d t, \quad y^b_n(t) = p(\tau)\cos\,\omega_d t \tag{8, 9}$$

and

$$y^a_{n-1}(t) = p(\tau)\sin\,\omega_d(t-1), \quad y^b_{n-1}(t) = p(\tau)\cos\,\omega_d(t-1). \tag{8′, 9′}$$

In Eqs. (2)–(9), t is time and $\delta\tau$ is the time increment or time step for the integration.

The selection of an analysis time-step was based on the calculated structural frequencies and the estimated structural response frequencies. A general rule is that the dynamic analyses time-step should be one-twentieth $\left(\frac{1}{20}\right)$ that of the inverse of the highest structural frequency under examination. For this particular problem, the time step $\delta\tau$ was chosen to be $\delta\tau = 0.005\,\mathrm{s}$. The

system-damping ratio ξ was determined to be $\xi = 0.003$, as this is an estimate of the typical average damping ratio that a cable-stayed bridge, such as the Second Severn Crossing, exhibits [17]. The duration of the signal τ varied, as various lengths of time-histories were used for the analyses of the response of the cable. The average time-history length is about $\tau = 120\,\text{s}$. Much longer time-histories were also used to examine whether or not a maximum cable displacement could occur beyond the two-minute mark. Fig. 2 represents a typical normal distribution white noise signal or linear system wind load. Fig. 3 represents the response of the linear system to the white noise (wind load), normalised to a unit of *one*. Fig. 4 shows the linear system frequency response, as calculated by the Duhamel integral. Figs. 5a and b represent system responses using alternative white noise signals. Figs. 3, 5a and b also represent typical synthetic stochastic cable support excitations, which were used for the analysis of the cables nonlinear response. In each of these figures, the dominant frequency represents the frequency at which the linear mass–spring–dashpot damper system was tuned to. Fig. 6 is a schematic of the procedure for the derivation of the synthetic stochastic input signals.

As has been previously mentioned, the cable was modelled using finite elements, which were then used to investigate regions of large-amplitude cable vibrations in a two-dimensional parameter space—excitation circular frequency Ω and a parameter β. In Ref. [15], parameter β is a function of the maximum amplitude of the sinusoidal support excitation and is defined by Eq. (10). Here β represents a similar quantity only that now it is a function of the maximum excitation amplitude that can be found throughout the synthetic stochastic time-history, i.e. the normalised synthetic stochastic time-history is multiplied by $\Delta_{\max}$. Several analyses for comparison, using like-for-like sinusoidal vs. stochastic root mean square (RMS) values, were also performed and

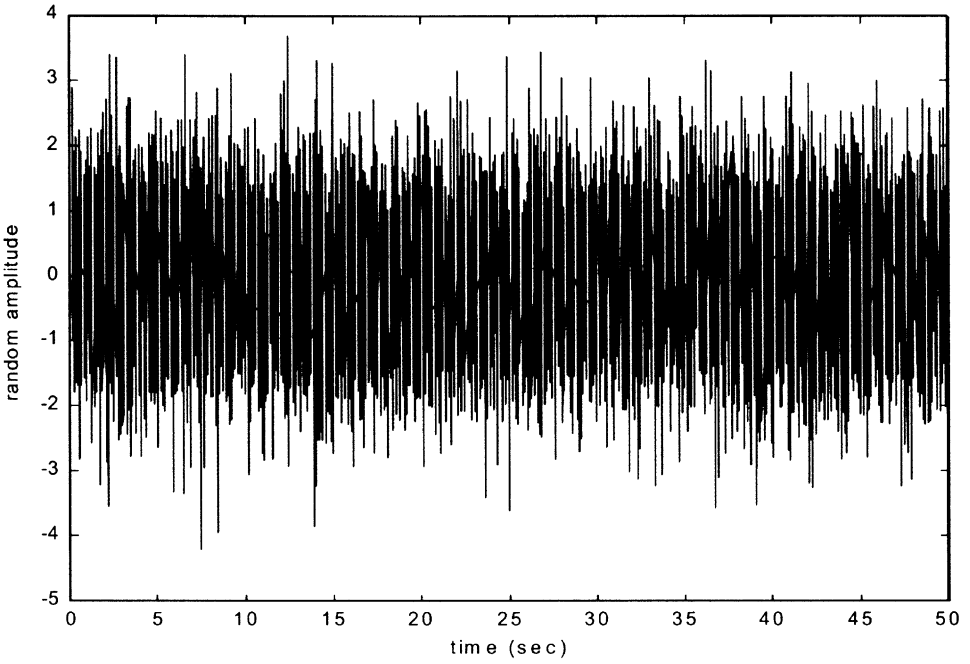

Fig. 2. Random normal distribution "white noise" signal.

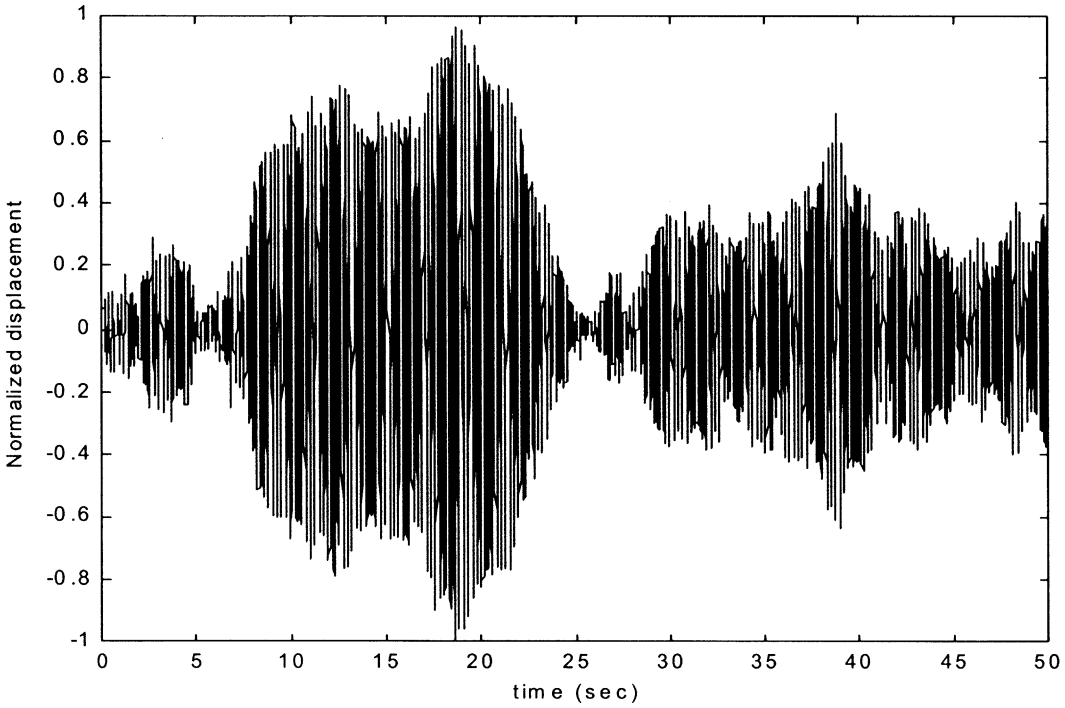

Fig. 3. Segment of nortmalised response of sdof structure used as stochastic input for cable A.

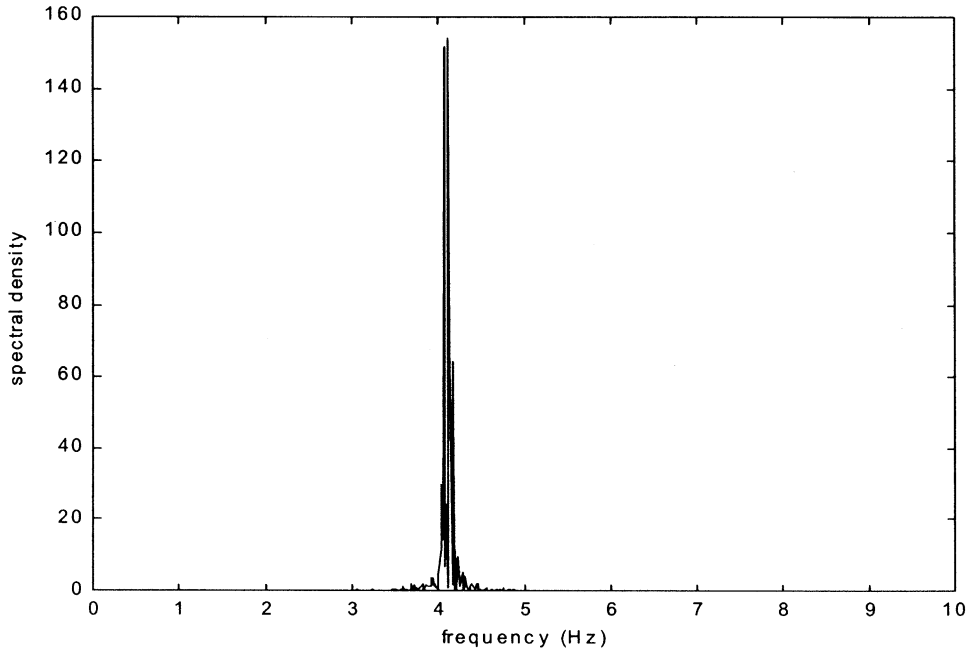

Fig. 4. Power spectra density of stochastic cable input signal for 4.087 Hz.

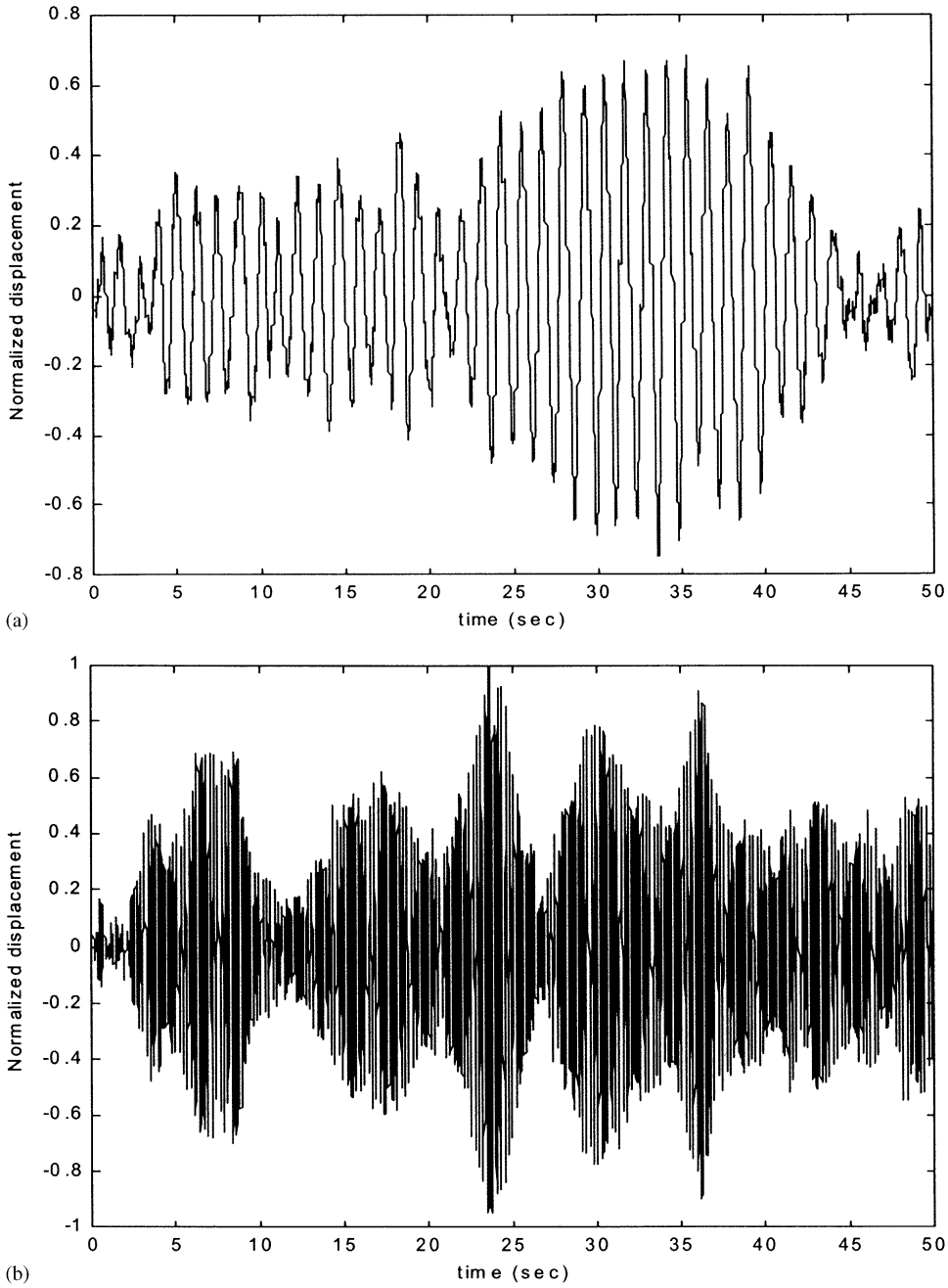

Fig. 5. (a) Segment of example synthetic stochastic record used for cable response analysis. (b) Segment of example synthetic stochastic record used for cable response analysis.

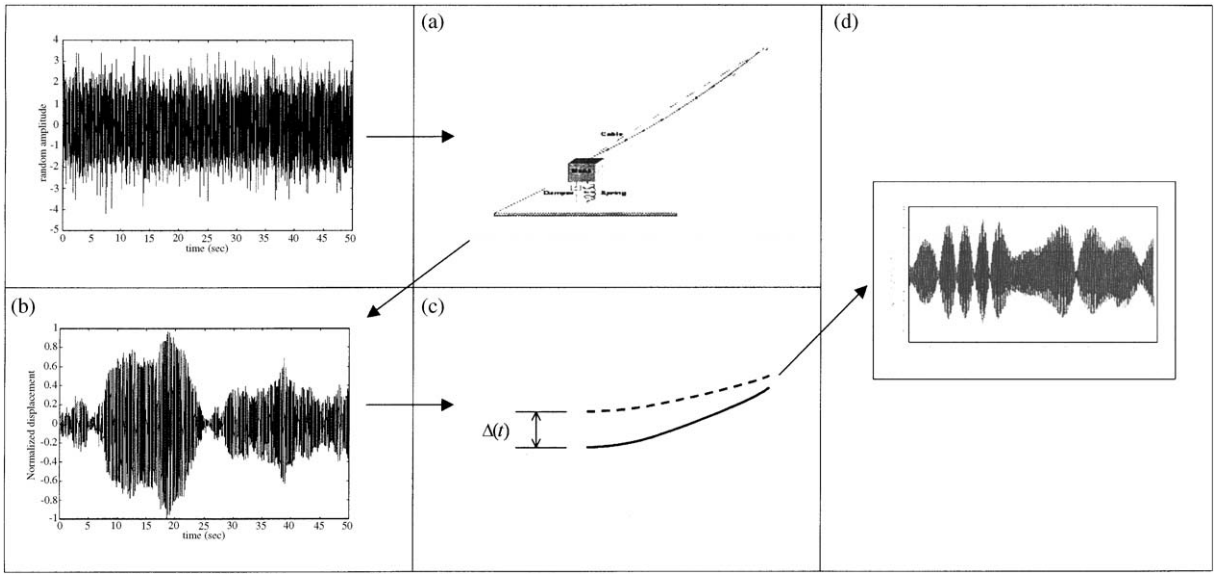

Fig. 6. Schematic of stochastic cable analysis procedure (a) "white noise" signal is filtered through sdof cable supported system with specific dynamic characteristics; (b) sdof produces desired synthetic response; (c) synthetic response is used on cable as synthetic stochastic support record; (d) final cable response is obtained.

are presented in a following section.

$$\beta = \left(\frac{5\pi\sqrt{EA/\mu}}{\omega_1}\right)\left(\frac{\Delta_{\max}}{l^2}\right). \tag{10}$$

Again, the coefficients of Eq. (10) are defined in the nomenclature.

4.2. Regions of large amplitude cable vibrations

To investigate the large-amplitude cable vibrations, in the parameter plane $\Omega-\beta$, two damping values for the cable were chosen. The structural damping of the cable is estimated, as previously mentioned, to be about 0.05%. A series of analyses with this value were performed with the synthetic stochastic time-histories and the results were then compared to those found from the analyses of the cable with both structural and aerodynamic damping.

Aerodynamic damping was calculated theoretically, according to Virlogeux [18]. When a cable is moving parallel to the wind, its aerodynamic damping can be found from the following equation:

$$\xi_{pk} = \rho V D C_d / 2\mu\omega_k, \tag{11}$$

where ρ is the air density (1.225 kg/m^3), V the wind velocity, C_d the drag coefficient, D the cable diameter, and ω_k the cable's linear modal frequencies. When the cable is moving normal to the

direction of the wind

$$\xi_{nk} = \rho V D C_d / 4\mu\omega_k. \tag{12}$$

A drag coefficient of $C_d = 1.2$ [17], for cable A (cable diameter is 0.25 m), is equivalent to the drag that the cable will have with a wind speed of about $5\,\mathrm{m\,s^{-1}}$. Table 1 shows the damping values found using these parameters and applying Eqs. (11) and (12).

Macdonald [21] estimated damping values for a cable with similar characteristics to cable A, from on-site measurements, and found that the cable's actual, normal to wind, damping ξ_{n1} is near 0.0015. This value is close to that found theoretically (0.00155) from Eq. (11) and this, together with the cable's structural damping, was used as the damping value for the analyses of the cable with structural and aerodynamic damping. As only negligible differences (~2%) in the cable's response, with this increase in damping, were observed, only the results from the analyses performed using only structural damping are presented.

As in Ref. [15], a much higher damping value of 3.3%, for cable A, was chosen for a third set of analyses. These were performed to investigate the effect that an extreme damping value would have on the cable's response. By considering extreme changes in the parameters that govern the aerodynamic damping of the cable, a larger cable damping value was found. The drag coefficient was increased from $C_d = 1.2$ to $C_d = 2.1$, for a wind velocity of $30\,\mathrm{m/s^{-1}}$, even though this is highly, unlikely as C_d tends to drop from $C_d = 1.2$ to $C_d = 0.4$ after a wind velocity of about $10\,\mathrm{m/s^{-1}}$. Revised increased damping values are also shown in Table 1. The implementation of both damping values within the FEA was achieved through the use of Rayleigh Damping.

As can clearly be seen from Fig. 7a, the analyses reveal regions of large-amplitude cable vibrations occurring at $\Omega = 0.5\omega_1^{\mathrm{nl}}$, $\Omega = 1.0\omega_1^{\mathrm{nl}}$, $\Omega = 1.3\omega_1^{\mathrm{nl}}$ and $\Omega = 2.0\omega_1^{\mathrm{nl}}$, for the stochastic cable support excitation input. These instabilities are very similar to those found when applying sinusoidal cable support excitation, as they occur at the same frequencies. Fig. 7b represents the response of the same cable with the same parameters under the influence of the sinusoidal cable support excitation, as determined by Georgakis et al. [15]. Greater differences between the regions of large-amplitude cable vibrations are found, though, when comparing out-of-plane cable responses to the applied stochastic and sinusoidal cable support excitations. Fig. 7c represents the out-of-plane response of the cable to a stochastic cable support excitation, while Fig. 7d represents the out-of-plane response of the same cable to a sinusoidal cable support excitation. Fig. 7c clearly shows that the cable can exhibit large-amplitude out-of-plane displacements at various circular excitation frequencies from between $\Omega = 0.0\omega_1^{\mathrm{nl}}$ and $\Omega = 2.3\omega_1^{\mathrm{nl}}$, when excited by a stochastic input, even though this does not occur for a sinusoidal input.

Figs. 8a–e show a one-to-one comparison between in-plane cable responses to varying sinusoidal and stochastic cable support excitations. Each one of these is for a given maximum excitation amplitude, $\Delta_{\max}$.

Table 1
Theoretical ξ damping values for cable A, applied in SOLVIA using Rayleigh damping

	ξ_p when cable velocity parallel to wind	ξ_n when cable velocity normal to wind
Low damping	0.00310	0.00155
High damping	0.0325	0.0163

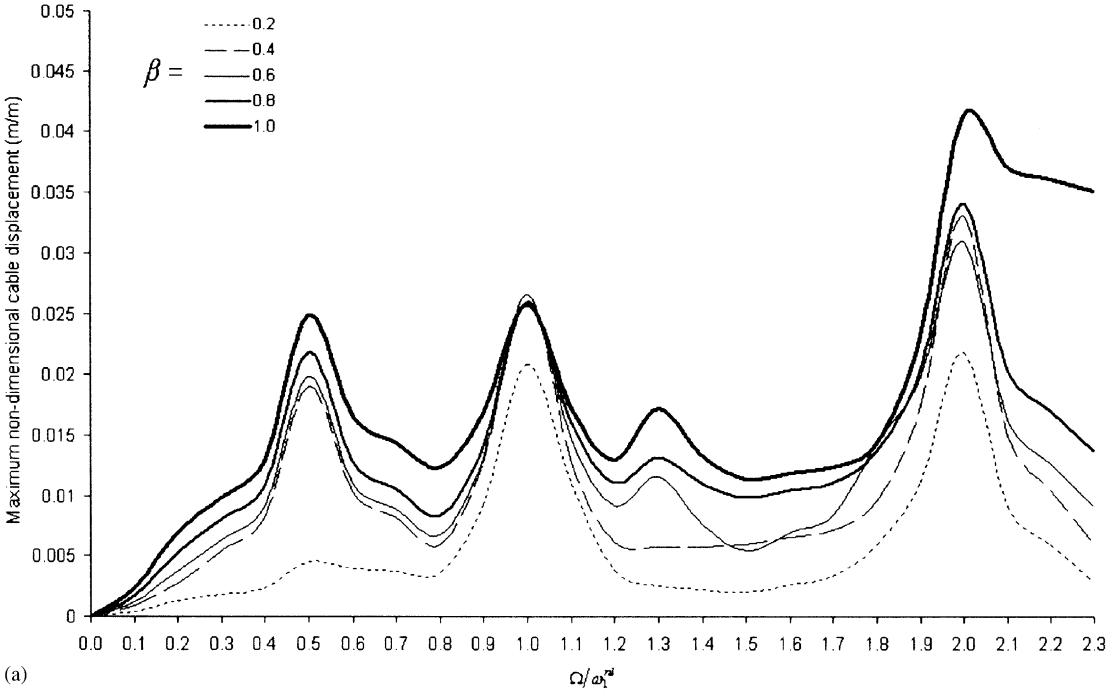

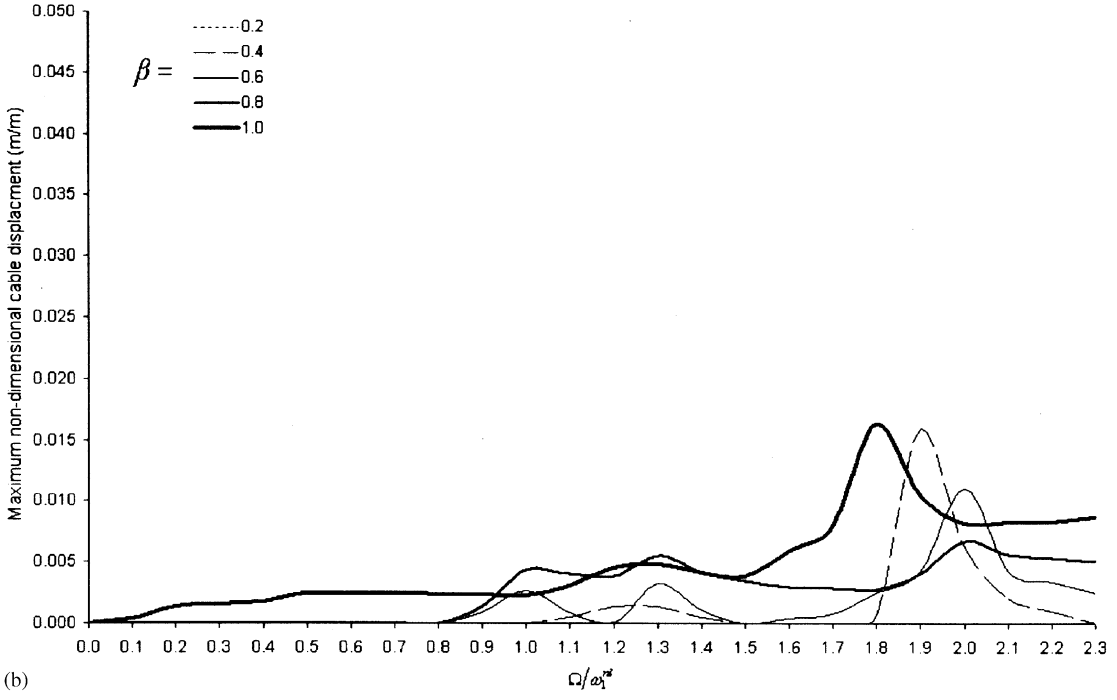

Fig. 7. (a) In-plane cable response to stochastic support excitation with $\xi = 0.05\%$, $\theta = 20.3^\circ$. (b) In-plane cable response to sinusoidal support excitation with $\xi = 0.05\%$, $\theta = 20.3^\circ$. (c) Out-of-plane cable response to sinusoidal support excitation with $\xi = 0.05\%$, $\theta = 20.3^\circ$. (d) Out-of-plane cable response to sinusoidal support excitation with $\xi = 0.05\%$, $\theta = 20.3^\circ$.

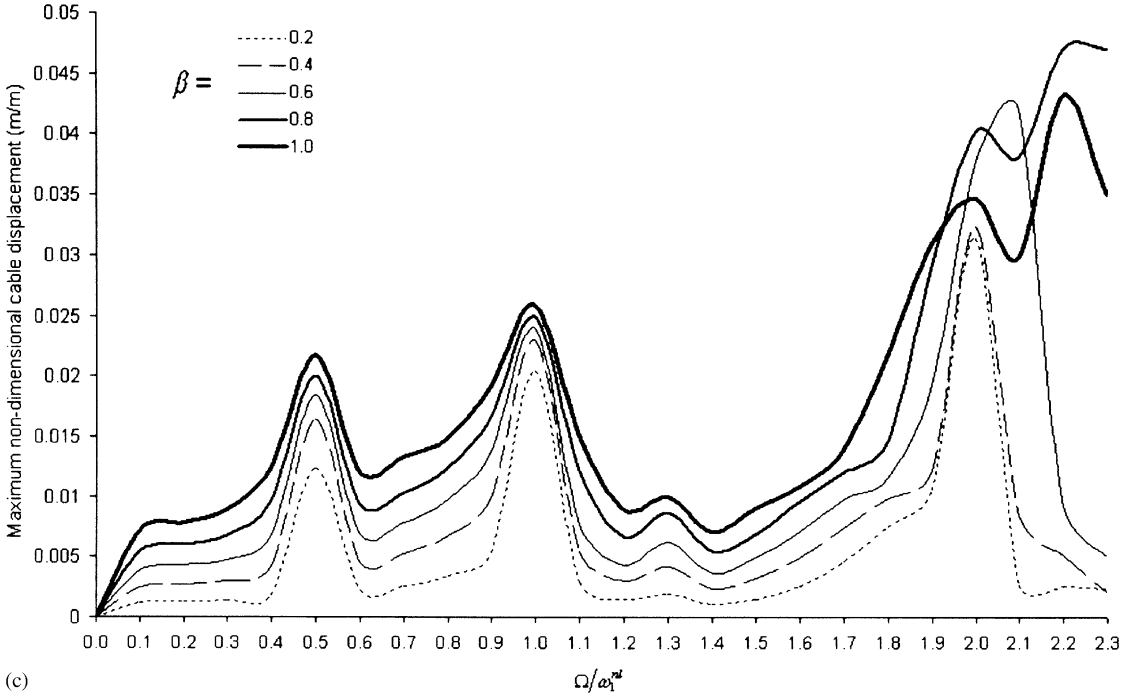

(c)

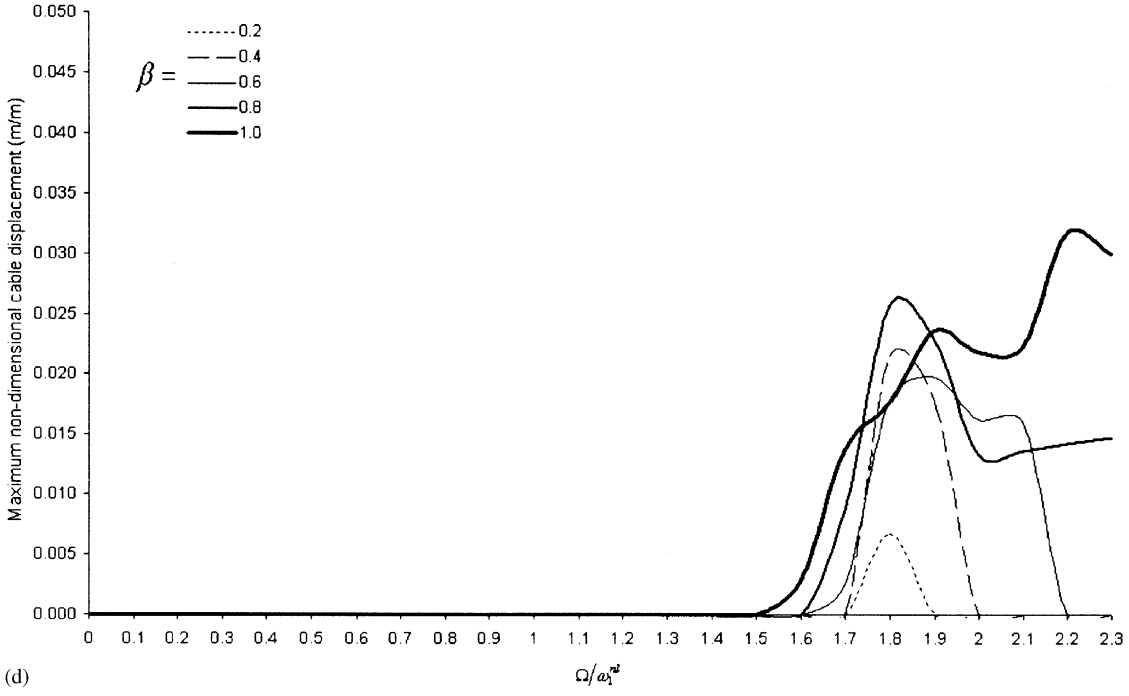

(d)

Fig. 7. (*Continued*)

Two main observations can be extracted from these comparisons. Firstly, cable vibration amplitudes, resulting from stochastic cable support excitation, are consistently larger than those resulting from sinusoidal cable support excitation, in the lower excitation frequencies ($\Omega = 0.0\omega_1^{nl} \rightarrow 1.6\omega_1^{nl}$). Also, cable vibration amplitudes resulting from stochastic cable support excitations are generally smaller than those resulting from sinusoidal cable support excitations in the higher excitation frequencies ($\Omega = 1.6\omega_1^{nl} \rightarrow 2.3\omega_1^{nl}$). Secondly, "cable-stiffening" does not occur for stochastic cable support excitations to the same degree as it does for sinusoidal cable support excitations [15], at the higher amplitude and higher frequency excitations. The second observation may be directly related to the first, in that cable-stiffening results from very large-amplitude cable vibrations. This is described in more detail in Section 7, below.

Figs. 9a–e show one-to-one comparisons between equivalent out-of-plane cable responses to sinusoidal and stochastic cable support excitations. These, again, are for a maximum given excitation amplitude Δ_{max}. The observations here are very similar to those extracted from the previous comparison. In the excitation frequency range $\Omega = 0.0\omega_1^{nl} \rightarrow 1.6\omega_1^{nl}$, out-of-plane cable displacements for the stochastic support excitations exist, where for the sinusoidal support excitations they do not. Also, in the frequency range $\Omega = 1.6\omega_1^{nl} \rightarrow 2.3\omega_1^{nl}$, maximum cable displacements are consistently larger for sinusoidal support excitation than for the stochastic support excitation. It is clear that the random nature of the cable's response, in combination with the random nature of the cable excitation at the higher excitation frequencies, does not allow the cable's out-of-plane parametric response to 'kick-in'. Longer duration steady-state excitations are necessary for the formation of a significant response, in the higher excitation frequencies. This is not the case for the lower excitation frequencies as cable is almost void of any kind of parametric out-of-plane response due to sinusoidal excitation.

4.3. High damping instabilities

The highly damped cable (3.3%) analyses also gave some very interesting results, which can be viewed by examining Figs. 10a and b. When comparing Figs. 10a and 7a it is evident that the higher damping acts in reducing total in-plane cable displacements significantly. Cable displacement reductions are similar for both stochastic and sinusoidal cable excitations. When comparing Figs. 10b and 7c, though, this reduction is not as evident. Again, for the excitation frequency range $\Omega/\omega_1^{nl} = 0.0 \rightarrow 1.6$, maximum out-of-plane cable displacements are reduced with an increase of damping, but for the excitation frequency range $\Omega/\omega_1^{nl} = 1.6 \rightarrow 2.3$, maximum cable displacements increase. This increase in maximum out-of-plane cable displacements with an increase in damping can be attributed to the effect that damping has on stabilising a cable's energy intake 'rhythm' by stabilising energy intake levels. With low levels of damping, less input energy is lost with every cycle. This, although, has the effect of destabilising the cables 'rhythm' by introducing sharp changes in energy levels. This is only true, though, for the extreme support excitation parameters of $\beta = 0.8$ and $\beta = 1.0$.

Note that Figs. 7a–10b were found using both gradually increasing transient stochastic and sinusoidal time-histories and abrupt transient stochastic and sinusoidal time-histories. No differences in the maximum cable displacement amplitudes were found between gradually increasing and abrupt transient time-histories.

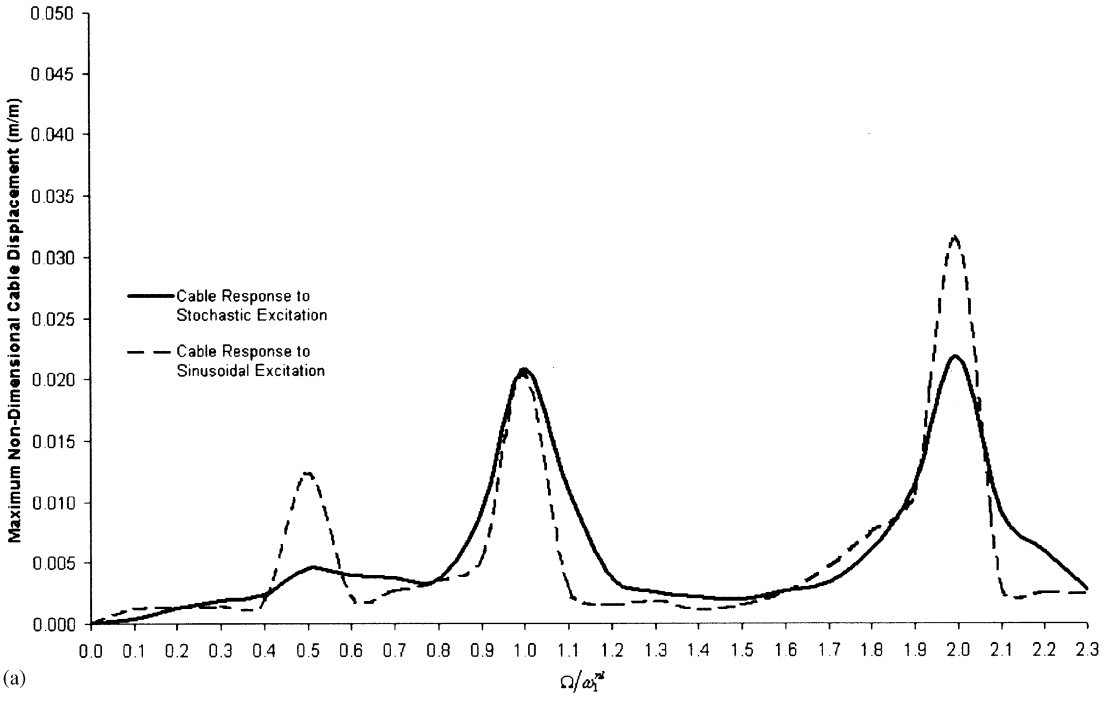

(a)

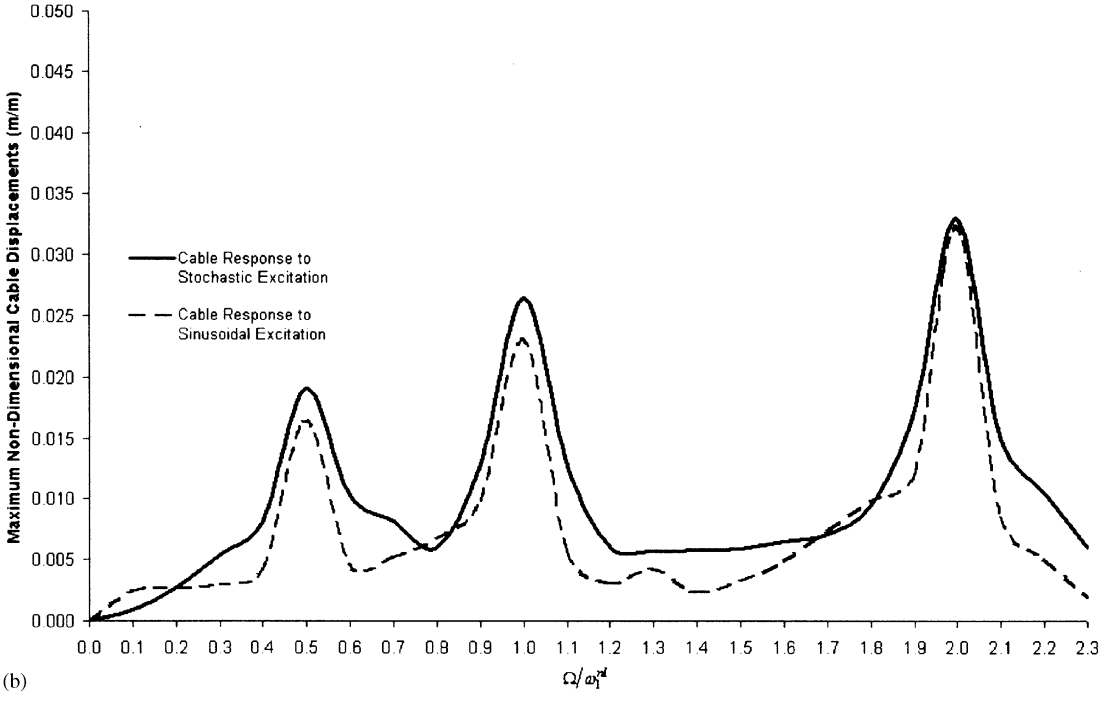

(b)

Fig. 8. (a) In-plane cable response to stochastic vs. sinusoidal excitation when $\beta = 0.2$, $\xi = 0.05\%$, $\theta = 20.3^\circ$. (b) In-plane cable response to stochastic vs. sinusoidal excitation when $\beta = 0.4$, $\xi = 0.05\%$, $\theta = 20.3^\circ$. (c) In-plane cable response to stochastic vs. sinusoidal excitation when $\beta = 0.6$, $\xi = 0.05\%$, $\theta = 20.3^\circ$. (d) In-plane cable response to stochastic vs. sinusoidal excitation when $\beta = 0.8$, $\xi = 0.05\%$, $\theta = 20.3^\circ$. (e) In-plane cable response to stochastic vs. sinusoidal excitation when $\beta = 1.0$, $\xi = 0.05\%$, $\theta = 20.3^\circ$.

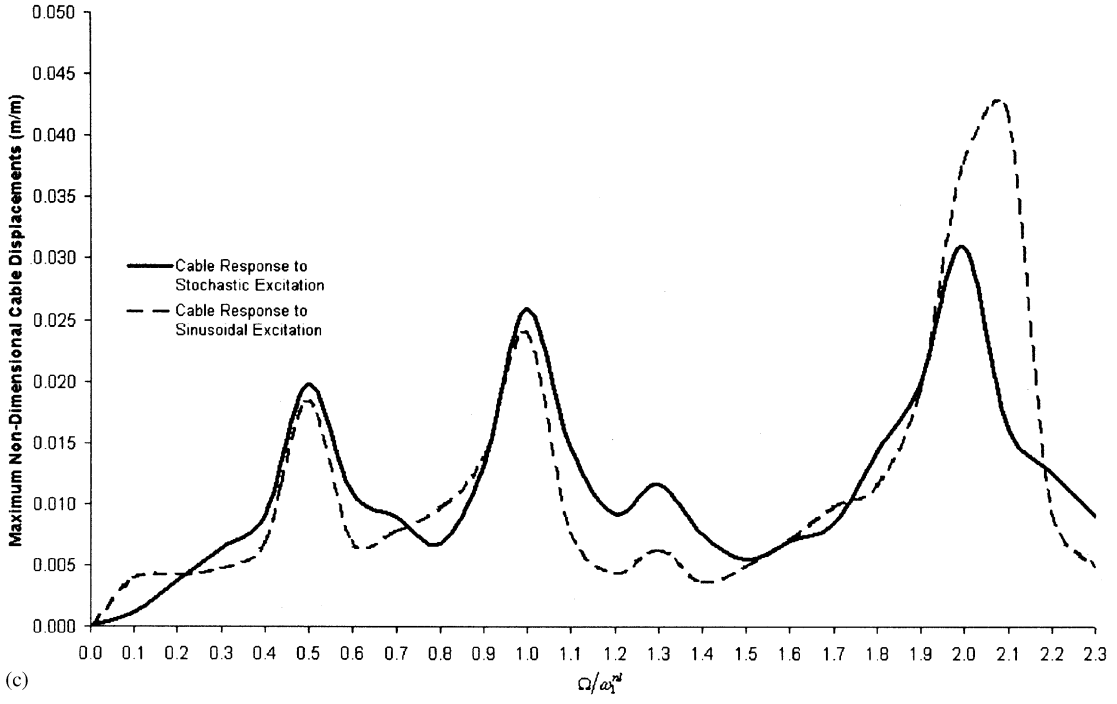

(c)

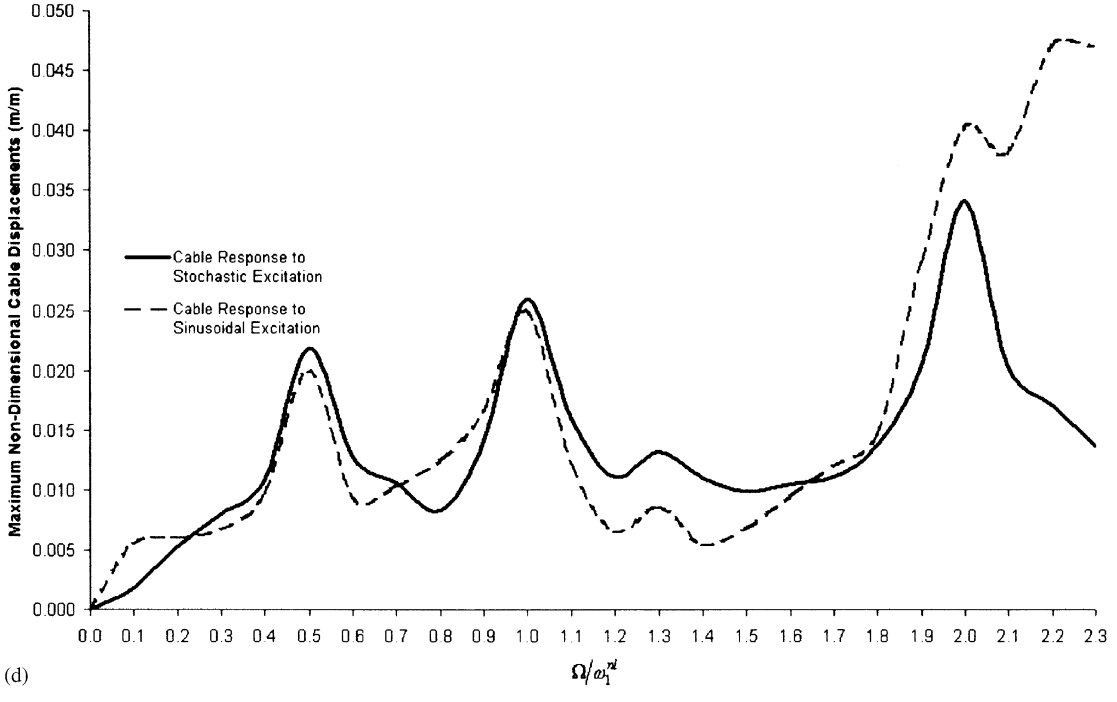

(d)

Fig. 8. (*Continued*)

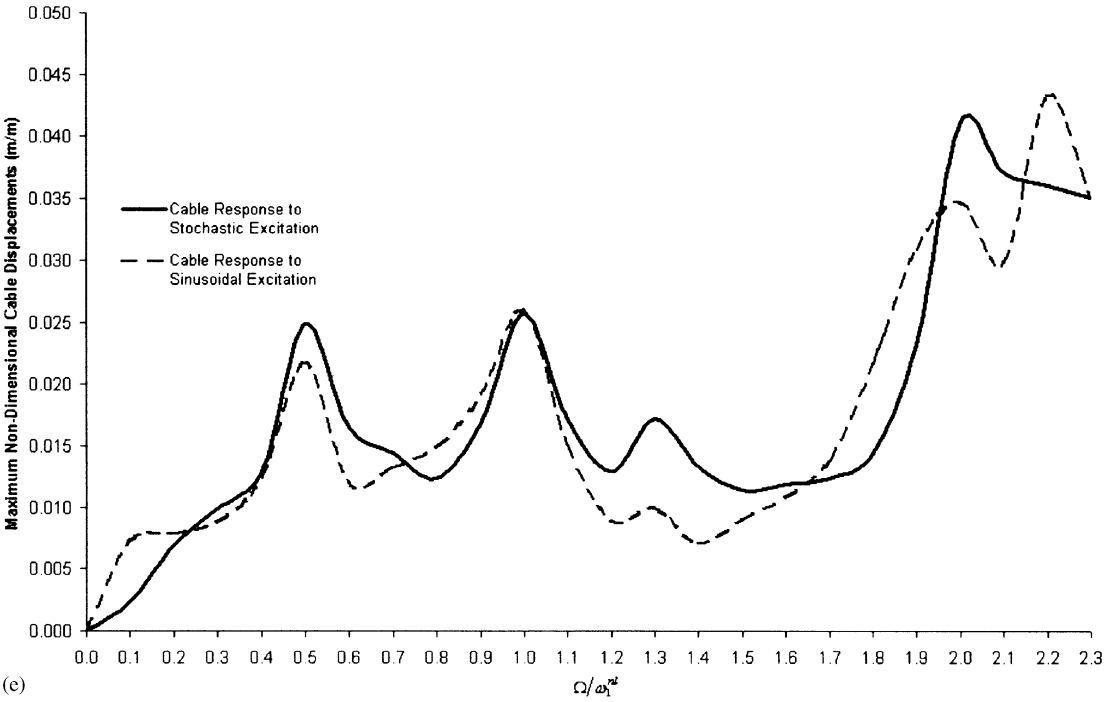

Fig. 8. (*Continued*)

4.4. Small stochastic cable support excitation

As in Ref. [15], a series of analyses was also performed to see what effects a very small stochastic cable support excitation ($\beta = 0.01$) had on the response of cable A. Fig. 11 represents the response of cable A to the small stochastic support excitation with both low (0.05%) and high (3.3%) levels of damping. Large-amplitude cable responses are concentrated around the excitation frequencies $\Omega = 1.0\omega_1^{nl}$ and $\Omega = 1.8\omega_1^{nl}$. Examining Fig. 11, one can note that at excitation frequencies $\Omega = 1.0\omega_1^{nl}$ and $\Omega = 1.8\omega_1^{nl}$, a maximum cable support displacement of $\beta = 0.01$, or $\Delta_{max} = 0.0000924$ m, for a 0.05% damped cable, will induce a cable response of approximately $u = 0.016$ and $u = 0.0044$ m, respectively. This is a ratio of 1:173.83 and 1:47.41, respectively. Thus, a bridge response, with an rms value equal to half of the maximum expected deck displacement of $\Delta_{max}^{bridge} = 0.01$ m, or 1 cm, at these frequencies, would induce maximum cable displacements (for a 0.05% damped cable) of about $u = 1.74$ and $u = 0.47$ m, respectively.

5. Effects of varying stochastic time-histories

The maximum cable response, to the stochastic cable support excitation, was calculated using several different stochastic time-histories. The maximum cable response can, in most cases, been found by measuring the maximum response of the cable to just one very long stochastic time-history, i.e. the maximum response from different time-histories, with the same β, Ω/ω_1^{nl} and rms

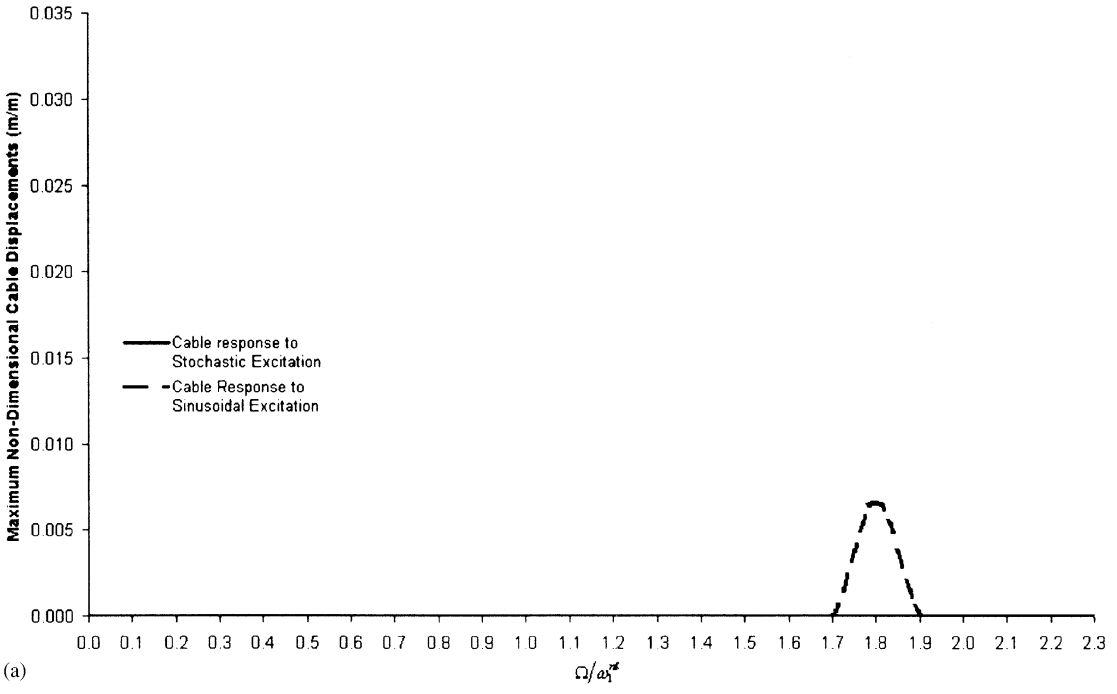

(a)

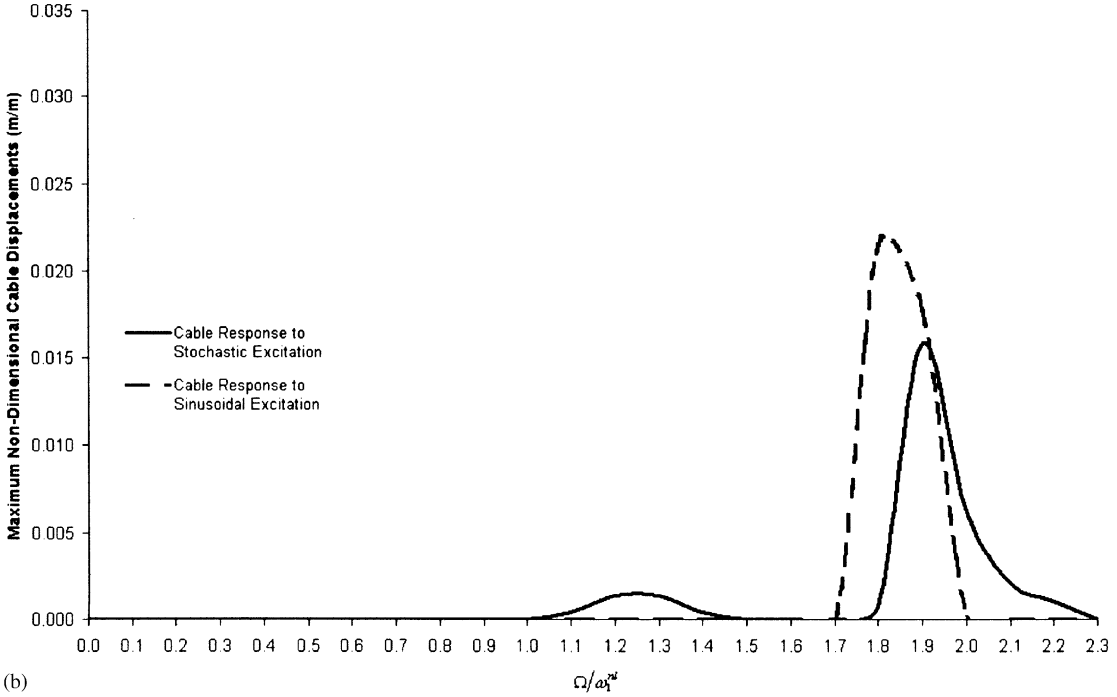

(b)

Fig. 9. (a) Out-of-plane cable response to stochastic vs. sinusoidal support excitation when $\beta = 0.2$, $\xi = 0.05\%$, $\theta = 20.3^\circ$. (b) Out-of-plane cable response to stochastic vs. sinusoidal support excitation when $\beta = 0.4$, $\xi = 0.05\%$, $\theta = 20.3^\circ$. (c) Out-of-plane cable response to stochastic vs. sinusoidal support excitation when $\beta = 0.6$, $\xi = 0.05\%$, $\theta = 20.3^\circ$. (d) Out-of-plane cable response to stochastic vs. sinusoidal support excitation when $\beta = 0.8$, $\xi = 0.05\%$, $\theta = 20.3^\circ$. (e) Out-of-plane cable response to stochastic vs. sinusoidal support excitation when $\beta = 1.0$, $\xi = 0.05\%$, $\theta = 20.3^\circ$.

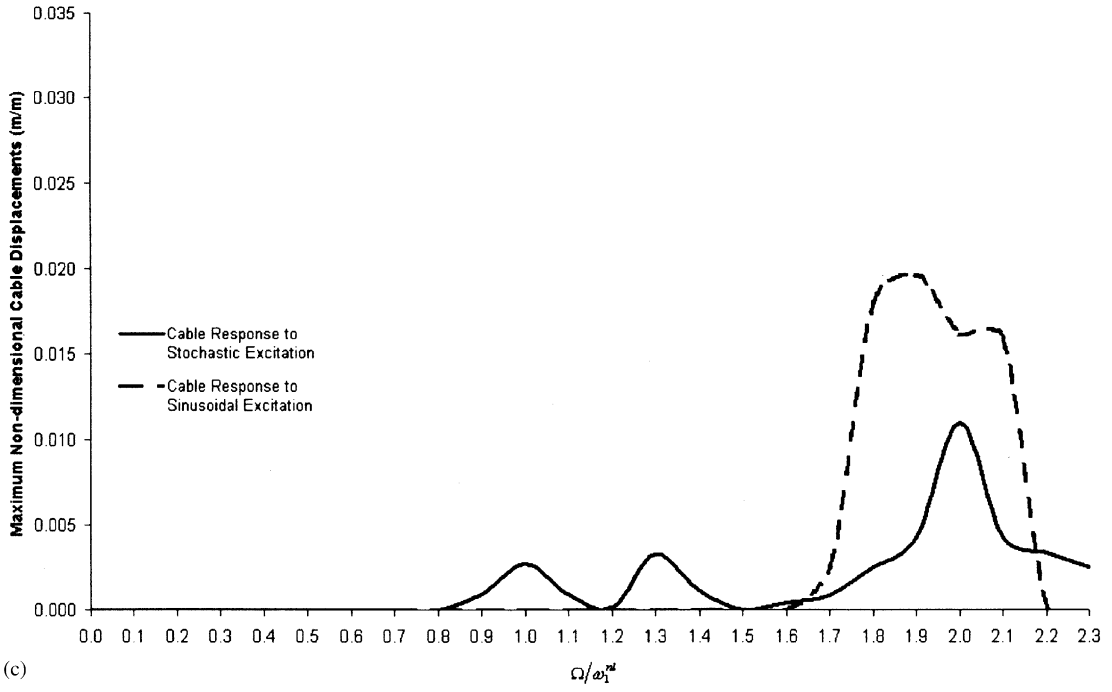

(c)

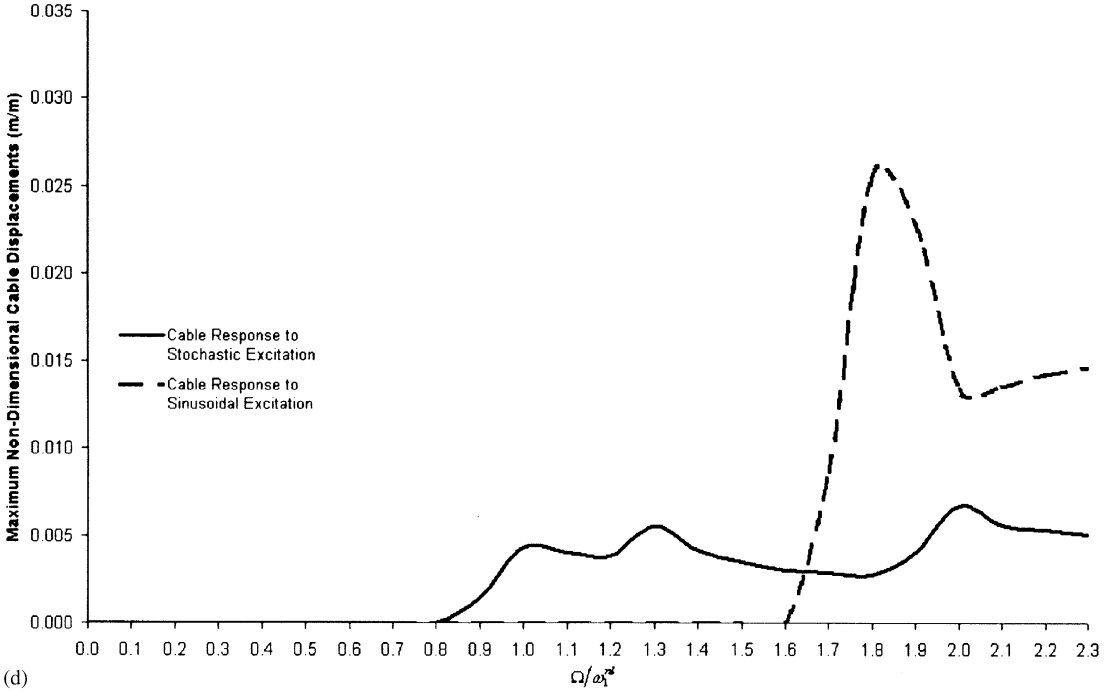

(d)

Fig. 9. (*Continued*)

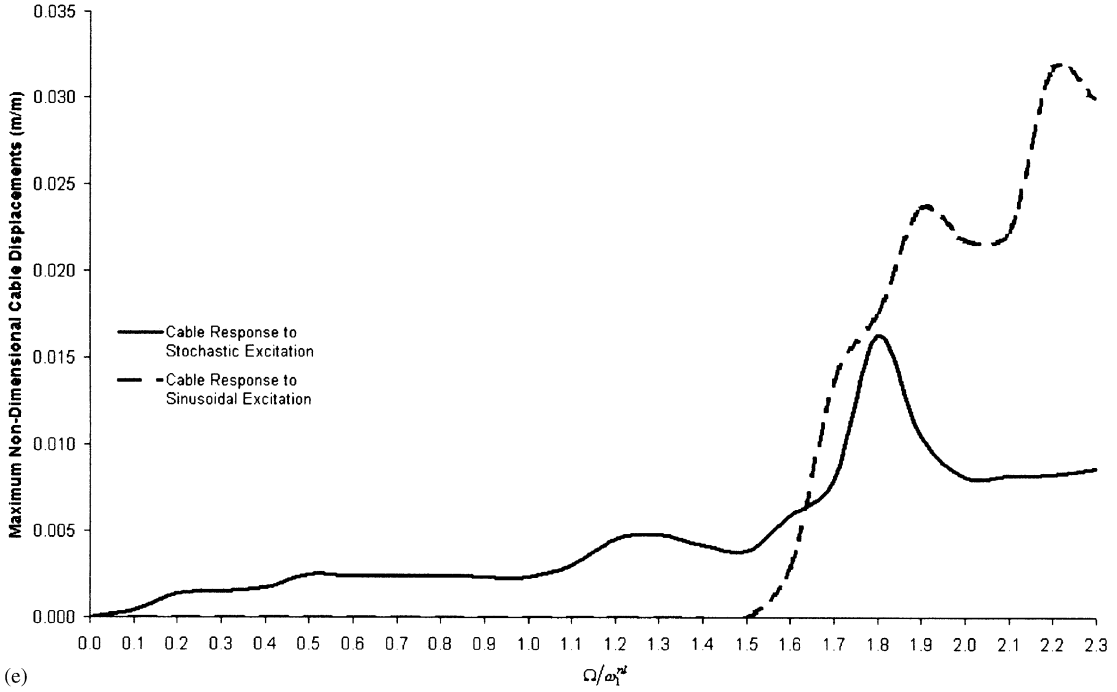

Fig. 9. (*Continued*)

values, was always the same. Thus, the effect of varying the stochastic time-histories, for the determination of cable response, is negligible if the stochastic time-history is long enough. As previously stated, it was found that the stochastic time-histories with a length $t = 120$ s were long enough to determine the maximum response of the cable.

6. Equivalent relative input energy

It is important to note that all of the previous stochastic vs. sinusoidal comparisons are made using cable responses to stochastic and sinusoidal time-histories, which have the same maximum cable end displacements, i.e. $\beta_{\text{stochastic}} = \beta_{\text{sinusoidal}}$. Even though the maximum level of excitation for each comparison is equal, the rms values of the support excitations are not. This means that the total "relative" input energy supplied by the stochastic support excitation is not equal to that supplied by the sinusoidal support excitation. A comparison between the total amount of relative input energy supplied by the stochastic and sinusoidal support excitations can be made by examining the rms levels of the respective time-histories. The stochastic time-history will produce a relative input energy E_i^{stoch}, which will be equal to the product of the sinusoidal relative signal's input energy E_i^{sin} and a relative energy coefficient e. Thus

$$E_i^{\text{stoch}} = eE_i^{\text{sin}}. \tag{13}$$

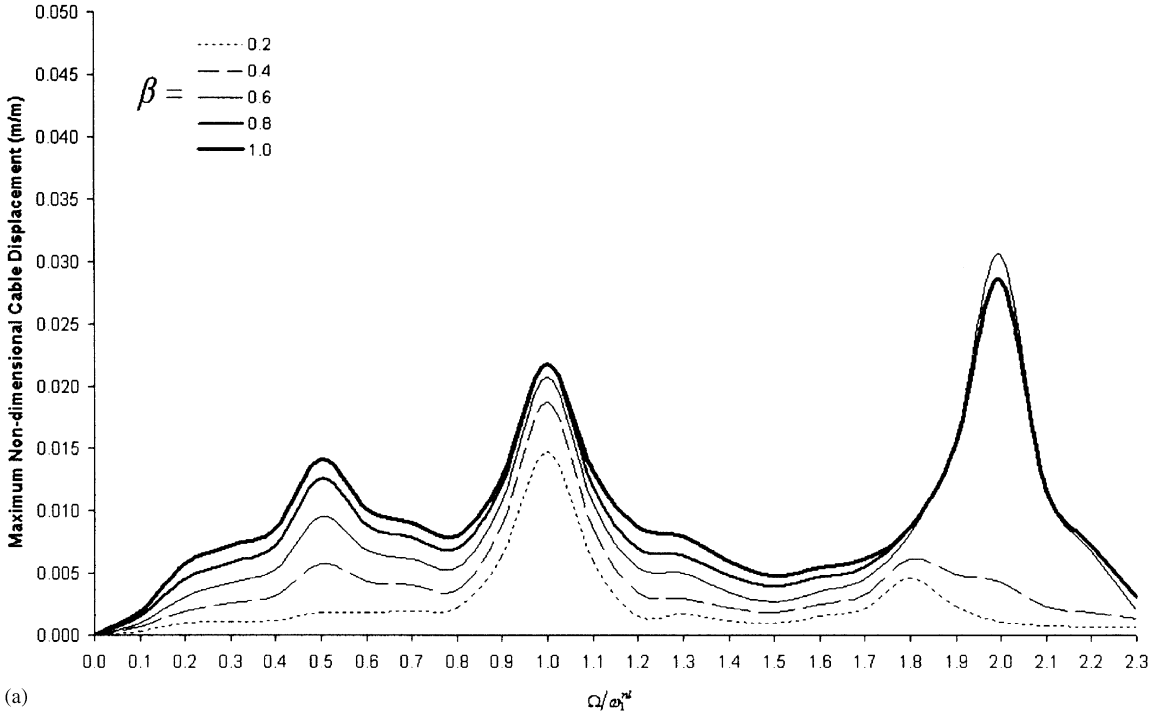

Fig. 10. (a) In-plane cable response to stochastic support excitation when $\xi = 3.3\%$, $\theta = 20.3^\circ$. (b) Out-of-plane cable response to stochastic support excitation with $\beta = 3.3\%$, $\theta = 20.3^\circ$.

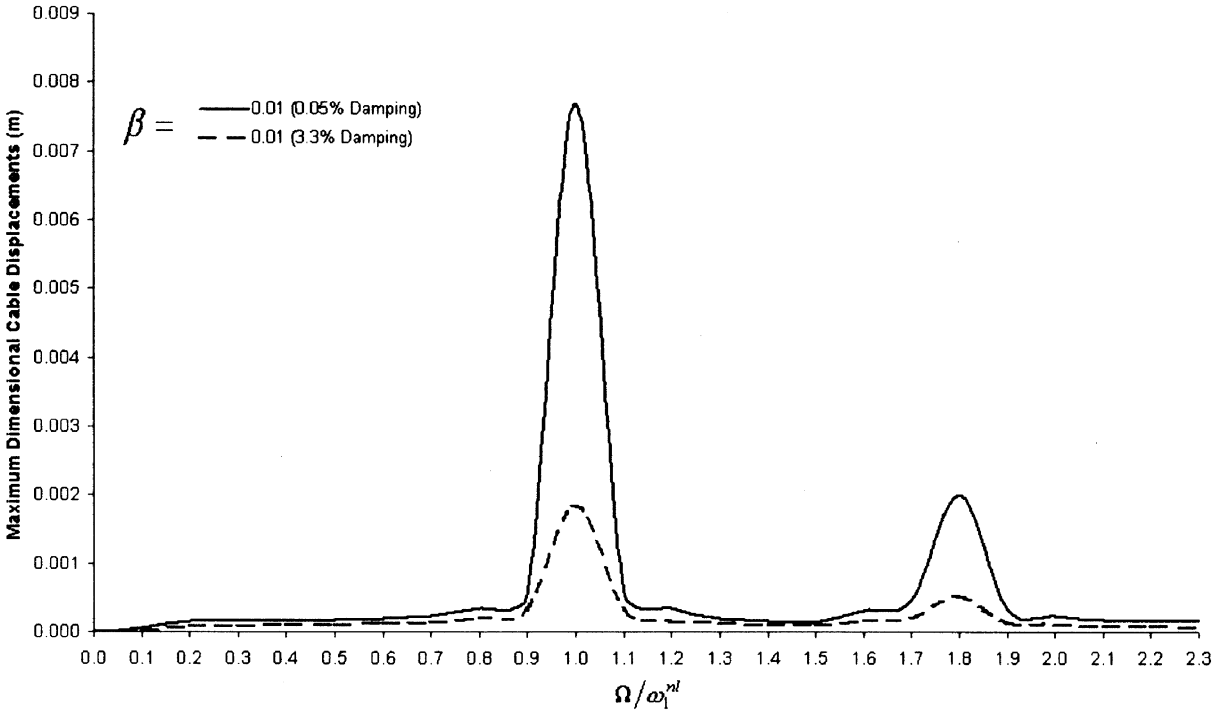

Fig. 11. In-plane cable response to low level stochastic support excitation with $\beta = 0.01$, $\xi = 0.05\%$ & 3.3%, $\theta = 20.3^{\circ}$.

It follows that if $e<1$, then the relative stochastic input energy will be less then that of the equivalent sinusoidal time-history, which has the same $\Delta_{\max}$ or β as that of the stochastic time-history; if $e>1$, then the opposite will be true.

Due to the inherent geometric nonlinearity of the cable under gravity, it is more appropriate to calculate the relative cable input energy by examining the energy of the linear mass–spring–dashpot damper system (Fig. 1), which acts as the cable's support. By examining the kinetic energy of the support, for both stochastic and sinusoidal support excitations, it is found that Eq. (13) also holds true for kinetic energies [21]. Thus

$$E_k^{\text{stoch}} = eE_k^{\text{sin}}, \tag{14}$$

where E_k^{stoch} and E_k^{sin} are the kinetic energies of the stochastic and sinusoidal support motions, respectively.

Manipulation of Eq. (14) leads to

$$e = \frac{(\Delta_{\text{rms}}^{\text{stoch}})^2}{(\Delta_{\text{rms}}^{\text{sin}})^2}, \tag{15}$$

where: $\Delta_{\text{rms}}^{\text{stoch}}$ and $\Delta_{\text{rms}}^{\text{sin}}$ are the stochastic and sinusoidal support excitation rms values, respectively.

Fig. 12 shows the average values of e for the above-mentioned (Section 4) stochastic vs. sinusoidal comparisons. As can be seen from Fig. 12, e is less than 0.3 throughout the excitation

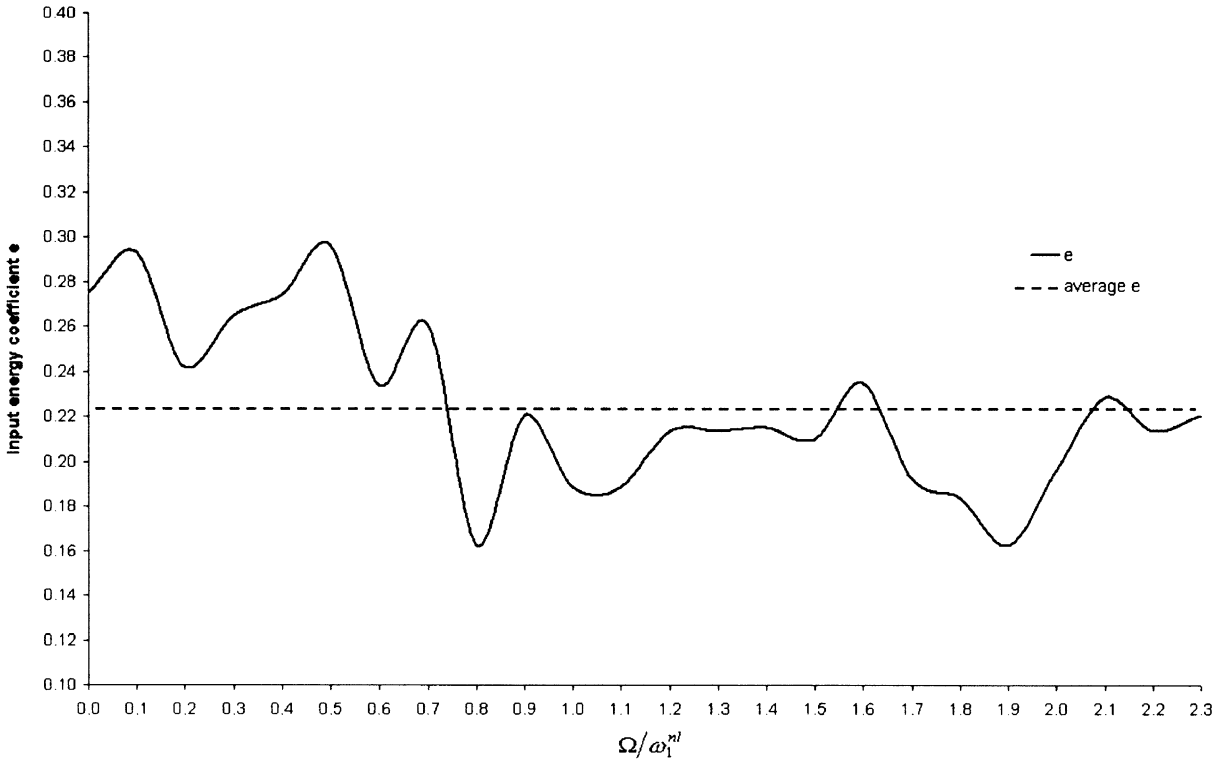

Fig. 12. Input energy coefficient e when $\beta_{\text{stochastic}} = \beta_{\text{sinusoidal}}$.

frequency range, i.e. the total relative stochastic input energy is always less than the compared sinusoidal input energy.

The one-to-one comparisons of Section 4 are valid in terms of maximum support displacements, but are not valid when comparing total relative stochastic vs. sinusoidal input energies. Thus, several critical parameter pairs within the excitation-forcing frequency ($\beta \leftrightarrow \Omega/\omega_1^{\text{nl}}$) parameter plane were chosen and analysed to measure what effect the stochastic support excitations would have on the cable's response, when $e = 1$ or $\Delta_{\text{rms}}^{\text{stoch}} = \Delta_{\text{rms}}^{\text{sin}}$. Fig. 13 shows a comparison of in-plane maximum cable stresses ratios, $\sigma_{\max}/\sigma_y$, obtained by analysing the response of the cable to stochastic support excitation time-histories when $\beta_{\text{stochastic}} = \beta_{\text{sinusoidal}}$ and $\Delta_{\text{rms}}^{\text{stoch}} = \Delta_{\text{rms}}^{\text{sin}}$.

Through examination of Fig. 13 it can be concluded that a comparison between cable responses from sinusoidal and stochastic support excitations is more appropriate when considering $\beta_{\text{stochastic}} = \beta_{\text{sinusoidal}}$. Even though stress levels within the cable are increased for both type of excitation level, it is clearly more reasonable, both in terms of displacement and stress levels, to compare cable responses to stochastic and sinusoidal support excitation when $\beta_{\text{stochastic}} = \beta_{\text{sinusoidal}}$.

As can be seen from Fig. 12, though, the relative input energy from the stochastic support excitations is 66 and 85% less than that found from the equivalent sinusoidal time-history, even

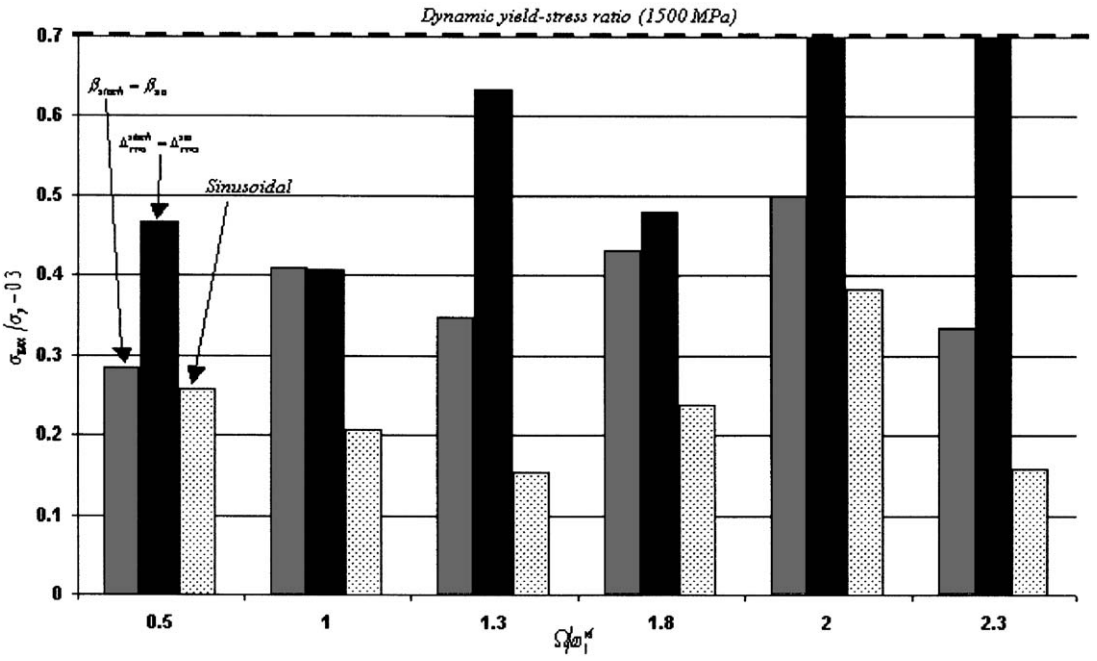

Fig. 13. Comparison of maximum cable stress ratios between sinusoidal and stochastic loading.

when $\beta_{\text{stochastic}} = \beta_{\text{sinusoidal}}$. This implies that a stochastic time-history that has between 66–85% less relative input energy than the equivalent sinusoidal time-history when $\beta_{\text{stochastic}} = \beta_{\text{sinusoidal}}$, can produce a maximum cable response that is equivalent or greater to that found from the sinusoidal time-history.

7. Cable stiffening

According to Georgakis et al. [15], cable stiffening was observed for higher amplitude cable displacements due to sinusoidal cable end displacements. Although this phenomenon is not as pronounced, here again there is an indication that cable stiffening does occur at the higher excitation frequencies $2.0\omega_1^{\text{nl}} \leqslant \Omega \leqslant 2.3\omega_1^{\text{nl}}$. This can be observed, especially for the higher amplitude support excitation of $\beta = 1.0$, as a higher than expected maximum cable displacement, for the prescribed excitation frequency.

8. Assumptions

All of the analyses were undertaken with the assumption that the cable stresses were always less than those required for material yielding ($\sigma_y = 1500\,\text{MPa}$) and, as such, the stresses were

continuously monitored. Unlike the analyses in Ref. [15], cable stresses, in these analyses, did manage, in a few cases, to reach and surpass the material yield stress. This did not occur for the analyses performed when considering $\beta_{\text{stochastic}} = \beta_{\text{sinusoidal}}$, but did occur at $\Omega = 2.0\omega_1^{\text{nl}}$ and $\Omega = 2.3\omega_1^{\text{nl}}$ for the analyses performed when $\Delta_{\text{rms}}^{\text{stoch}} = \Delta_{\text{rms}}^{\text{sin}}$ and $\beta = 0.5$.

Additionally, it has been assumed that the support is not affected by the cable's response, but this may not necessarily be true. It is important that a cable's support or end mass is quantified to determine whether the cable has an influence over the support excitation or not. If the support mass is sufficiently larger than that of the cable, the cable will have little or no influence on the support and its excitation. A support mass to cable mass ratio of 500:1 or greater was found to be enough to avoid the more significant effects of cable–support interaction. The effects of this interaction, although, are examined in greater detail by Georgakis [22].

9. Concluding remarks

Even though sinusoidal cable support excitation is relevant and real in actual structures, stochastic cable support excitation occurs more frequently. While the response of a cable to sinusoidal cable support excitation has been studied in detail by the current authors and other researchers in the past, research into the response of a cable to stochastic cable support excitation seems to have been left wholly untouched.

Results from the analyses of the response of a cable to stochastic support excitation are interesting. For low structural and aerodynamic damping (0.05–0.15%), the cable's maximum in-plane displacements are very similar, both in amplitude and in pattern, to those found from analyses using sinusoidal cable support excitation. Large-amplitude cable vibrations tend to occur at the specific excitation frequencies of $\Omega = 0.5\omega_1^{\text{nl}}$, $\Omega = 1.0\ \omega_1^{\text{nl}}$, $\Omega = 1.3\omega_1^{\text{nl}}$, $\Omega = 1.8\omega_1^{\text{nl}}$ and $\Omega = 2.0\omega_1^{\text{nl}}$. Out-of-plane displacements are very different, though. For the excitation circular frequency range of $0.0\omega_1^{\text{nl}} < \Omega < 1.6\omega_1^{\text{nl}}$, out-of-plane cable displacements exist and are fairly significant, especially when compared to those found using sinusoidal cable support excitations. For the excitation circular frequency range of $1.6\omega_1^{\text{nl}} < \Omega < 2.3\omega_1^{\text{nl}}$, out-of-plane cable displacements resulting from stochastic cable support excitation are consistently smaller than those found resulting from sinusoidal cable support excitation.

Higher aerodynamically damped (3.3%) cable response analyses showed that the in-plane response of the cable to stochastic support excitation is very similar to the cable's response to sinusoidal cable support excitation. The out-of-plane response of the cable resulting from stochastic support excitation was also similar to that resulting from sinusoidal support excitation, with the higher levels of damping. When comparing the high vs. low damping cable responses to stochastic support excitation, it was found that while the higher damping reduced out-of-plane displacements in the lower excitation frequencies, it actually increased out-of-plane cable displacements in the higher excitation frequencies.

Comparisons of in-plane and out-of-plane cable responses to stochastic and sinusoidal support excitations should in most cases be undertaken using like-for-like maximum support displacements ($\beta_{\text{stochastic}} = \beta_{\text{sinusoidal}}$) and not like-for-like rms values ($\Delta_{\text{rms}}^{\text{stoch}} = \Delta_{\text{rms}}^{\text{sin}}$). It is important to note that even when $\beta_{\text{stochastic}} = \beta_{\text{inusoidal}}$, a stochastic cable end displacement with a relative input energy, which is between three to six times smaller than the equivalent relative

sinusoidal input energy, can induce a maximum cable response that can be equal to or greater than that which can be induced by an equivalent sinusoidal input time-history.

Cable stiffening does occur for stochastic cable support excitations at higher excitation frequencies, but to a lesser extent than for higher amplitude and higher frequency sinusoidal cable support excitations.

Finally, it was found that, very large cable vibrations can occur for very small cable support displacements and can (due to a cable's low inherent damping) continue, even after the initiating support excitation (cable end displacements) have subsided. One unit of support displacement can lead to an in-plane cable displacement of up to 174 units.

References

[1] A.G. Davenport, A simple representation of the dynamics of a massive stay cable in the wind, *Proceedings of the International Conference of Cable-Stayed and Suspension Bridges (AFPC)*, Vol. 2, Deauville, 1994, pp. 427–438.

[2] C. Verwiebe, Rain-wind induced vibrations of cables and bars, in: A. Larsen, S. Esdahl (Eds.), *Bridge Aerodynamics*, Balkema, Rotterdam, 1998, pp. 255–263.

[3] M. Matsumoto, N. Shiraishi, H. Shirato, Rain-wind induced vibration of cables of cable-stayed bridges, *Proceedings of the Eighth International Conference on Wind Engineering*, London, Canada, 1991.

[4] M. Masumoto, Observed behaviour of prototype cable vibration and its generation mechanism, in: A. Larsen, S. Esdahl (Eds.), *Bridge Aerodynamics*, Balkema, Rotterdam, 1998.

[5] H.M. Irvine, T.K. Cauchey, The linear theory of free vibrations of a suspended cable, *Proceedings of the Royal Society of London A* 341 (1974) 299, 315.

[6] H.M. Irvine, *Cable Structures*, MIT Press, Cambridge, MA, 1981.

[7] K. Takahashi, Y. Konishi, Non-linear vibrations of cables in three dimensions—part I: non-linear free vibrations, *Journal of Sound and Vibration* 118 (1) (1987) 69–84.

[8] K. Takahashi, Y. Konishi, Non-linear vibrations of cables in three dimensions, part II: out-of-plane vibrations under in-plane sinusoidally time-varying load, *Journal of Sound and Vibration* 118 (1) (1987) 85–97.

[9] Y. Fujino, P. Warnitchai, B.M. Pacheco, An experimental and analytical study of autoparametric resonance in a 3DOF model of a cable-stayed-beam, *Nonlinear Dynamics* 4 (1993) 111–138.

[10] P. Warnitchai, Y. Fugino, T. Susumpow, A non-linear dynamic model for cables and its application to a cable-structure system, *Journal of Sound and Vibration* 187 (4) (1995) 695–712.

[11] H. Yamaguchi, Y. Fujino, Stayed cable dynamics and its vibration control, in: A. Larsen, S. Esdahl (Eds.), *Bridge Aerodynamics*, Balkema, Rotterdam, 1998, pp. 235–255.

[12] J.L. Lilien, A. Pinto da Costa, Vibration amplitudes caused by parametric excitation of cable stayed structures, *Journal of Sound and Vibration* 174 (1) (1994) 69–90.

[13] A. Pinto da Costa, J.A.C. Martins, F. Branco, J.L. Lilien, Oscillations of bridge stay cables induced by periodic motions of deck and/or towers, *Journal of Engineering Mechanics* 122 (1996) 613–622.

[14] N.C. Perkins, Modal interactions in the non-linear response of elastic cables under parametric external excitation, *International Journal of Non-Linear Mechanics* 27 (2) (1992) 233–250.

[15] C.T. Georgakis, C.A. Taylor, Nonlinear dynamics of cable stays. Part 1: sinusoidal support excitation, *Journal of Sound and Vibration* 281 (3–5) (2005) 537–564, this issue, doi:10.1016/j.jsv.2004.01.022.

[16] E.L. Mathieu, *Dynamique Analytique*, Gauthier-Villars, Paris, 1878.

[17] J.H.G. Macdonald, Identification of the Dynamic Behaviour of a Cable-stayed Bridge from Full-scale Testing during and after Construction, Ph.D. thesis, Department of Civil Engineering, University of Bristol, 2000.

[18] M. Virlogeux, Cable vibrations in cable-stayed bridges, in: A. Larsen, S. Esdahl (Eds.), *Bridge Aerodynamics*, Balkema, Rotterdam, 1998, pp. 213–233.

[19] SOLVIA95—SOLVIA Finite Element System, SOLVIA Engineering AB, Trefasgatan 3, SE-721 Västerås, Sweden, July 1996.
[20] R.W. Clough, J. Penzien, *Dynamics of Structures*, second ed, McGraw-Hill, New York, 1993.
[21] C.-M. Uang, V.V. Bertero, Evaluation of seismic energy in structures, *Earthquake Engineering and Structural Dynamics* 19 (1990) 77–90.
[22] C.T. Georgakis, Non-linear Dynamics of Cable Stays and Cable-Structure Interaction, Ph.D. Thesis, Departments of Civil and Aerospace Engineering, University of Bristol, 2001.